Hyperuniformity in 1D Quasiperiodic Point Patterns

Numerical Extraction of the Scaling Exponent via Diffusion Spreadability

Presented to Professor Salvatore Torquato

Princeton University

February 25, 2026

Hyperuniformity in 1D Quasiperiodic Point Patterns
Numerical Extraction of the Scaling Exponent via Diffusion Spreadability
Presented to Professor Salvatore Torquato
Princeton University
February 25, 2026

This presentation covers four completed phases of the 1D hyperuniformity project: code validation, pattern generation, real-space variance analysis, and reciprocal-space spreadability analysis. The main result is the numerical confirmation that $\alpha = 3$ universally for all metallic-mean substitution tilings.

Outline

Outline

1. Background
2. Phase 1: Code Validation
3. Phase 2: Pattern Generation
4. Phase 3: Real-Space Analysis
5. Phase 4: Two-Phase Media & Spreadability
6. Technical Challenges
7. Summary & Future Work

What Is Hyperuniformity?

A point pattern is **hyperuniform** if local number fluctuations are *suppressed* relative to random:

$$\sigma^2(R) \sim R^{d-\alpha}, \qquad S(k) \sim |k|^\alpha \text{ as } k \to 0$$

Class	Exponent	Variance growth	Examples
I	$\alpha > 1$	R^{d-1} (surface area)	crystals, quasicrystals
II	$\alpha = 1$	$R^{d-1} \ln R$	period-doubling chains
III	$0 < \alpha < 1$	$R^{d-\alpha}$	certain aperiodic chains

Goal: numerically extract α for three 1D quasicrystal families and verify $\alpha = 3$.

Challenge: dense Bragg peaks make direct $S(k)$ measurement impossible $\implies$ use *diffusion spreadability* (Torquato, 2021).

What Is Hyperuniformity?
A point pattern is **hyperuniform** if local number fluctuations are *suppressed* relative to random:
$\sigma^2(R) \sim R^{d-\alpha}, \qquad S(k) \sim |k|^\alpha$ as $k \to 0$
Class Exponent Variance growth Examples
I $\alpha > 1$ R^{d-1} (surface area) crystals, quasicrystals
II $\alpha = 1$ $R^{d-1} \ln R$ period-doubling chains
III $0 < \alpha < 1$ $R^{d-\alpha}$ certain aperiodic chains
Goal: numerically extract α for three 1D quasicrystal families and verify $\alpha = 3$.
Challenge: dense Bragg peaks make direct $S(k)$ measurement impossible $\implies$ use *diffusion spreadability* (Torquato, 2021).

Hyperuniformity was introduced by Torquato & Stillinger (2003). The key idea: for a Poisson process $\sigma^2 \sim R^d$ (volume scaling), while hyperuniform systems grow *slower*. The exponent α classifies how much slower. Class I ($\alpha > 1$) is the strongest form, with variance scaling like the surface area of the window.

The "measurement problem" for quasicrystals motivates the two-phase media / spreadability approach that is the heart of Phase 4.

The Three Metallic-Mean Quasicrystal Chains

Chain	Rule	Matrix M	Metallic mean μ	ρ
Fibonacci	$S \to L,\ L \to LS$	$\left(\begin{smallmatrix}0&1\\1&1\end{smallmatrix}\right)$	$\tau \approx 1.618$	0.724
Silver	$S \to L,\ L \to LLS$	$\left(\begin{smallmatrix}0&1\\1&2\end{smallmatrix}\right)$	$\mu_2 \approx 2.414$	0.500
Bronze	$S \to L,\ L \to LLLS$	$\left(\begin{smallmatrix}0&1\\1&3\end{smallmatrix}\right)$	$\mu_3 \approx 3.303$	0.361

Theoretical prediction (eigenvalue formula):

$$\alpha = 1 - \frac{2 \ln |\lambda_2|}{\ln \lambda_1}$$

Since $\det(\mathbf{M}) = -1$ for all three $\implies |\lambda_2| = 1/\lambda_1 \implies \boxed{\alpha = 3 \ \ \textbf{(universal)}}$

Tile lengths: $S = 1,\ L = \mu$. Production chains: $N \sim 10^7$ tiles.

Each chain is defined by a 2×2 substitution matrix acting on tile counts $[n_S, n_L]$. The eigenvalues determine both the growth rate (largest eigenvalue $\lambda_1 = \mu$) and the hyperuniformity exponent via the second eigenvalue.

Because $\det(\mathbf{M}) = -1$ for all metallic-mean matrices, $|\lambda_2| = 1/\mu$, giving $\alpha = 1 + 2 = 3$ universally. This is a purely algebraic result — our job is to verify it numerically.

Figure 1: Poisson Variance Benchmark

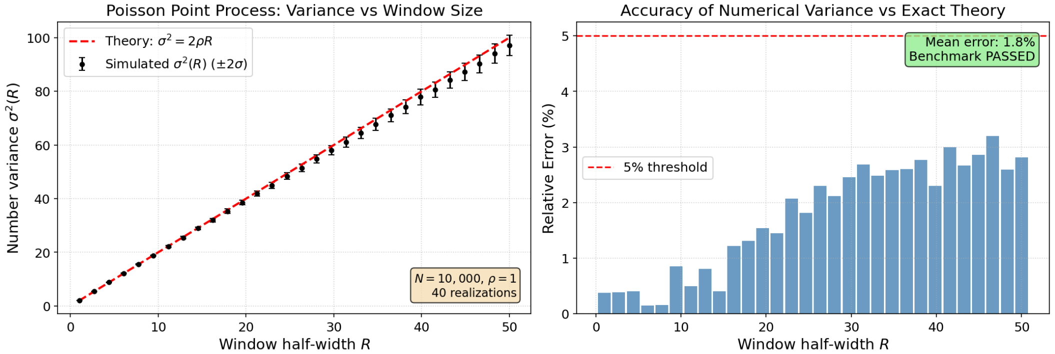

Figure 1: Code Validation — Poisson number variance matches exact result $\sigma^2 = 2\rho R$

Exact result $\sigma^2 = 2\rho R$ reproduced to 1.8% mean error $\implies$ sliding-window algorithm **validated**.

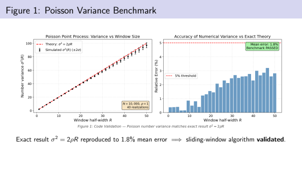

What this shows: We generate 40 independent Poisson point patterns (N=10,000, ρ=1) and compute $\sigma^2(R)$ via binary-search sliding windows.

Left panel: Computed variance (black dots $\pm 2\sigma$) vs. exact theory $\sigma^2 = 2\rho R$ (red dashed).

Right panel: Relative error at each R, all below 5%. Green box shows mean error = 1.8%.

Why it matters: This same algorithm is used for all subsequent variance computations. Validating it against the Poisson exact result ensures we can trust the quasicrystal measurements.

Two Independent Generation Methods

Method 1: Substitution

- Iterate substitution rules from seed L
- 34 iterations $\Rightarrow$ Fibonacci N=14,930,352
- Generates 10^7 tiles in $\sim$1 s
- Exactly 2 distinct spacings (verified)

Method 2: Cut-and-Project

- Embed $\mathbb{Z}^2$ lattice
- Strip of width ω along slope $1/\mu$
- Project interior points onto 1D line
- $\omega = \mu$: Class I; $\omega \neq \mu$: Class II

Both methods produce the **same quasicrystal** (up to rescaling), allowing cross-validation of $\bar{\Lambda}$.

Chain	Density ρ	Spacing ratio L/S
Fibonacci	0.7236	$\tau \approx 1.618$
Silver	0.5000	$\mu_2 \approx 2.414$
Bronze	0.3613	$\mu_3 \approx 3.303$

The substitution method is conceptually simple: start with L, apply the rule, repeat. The cut-and-project method provides an independent realization at a different density, which is crucial for verifying the rescaling invariance of $\bar{\Lambda}$.

Key point: substitution gives $\rho \approx 0.72$ for Fibonacci while projection gives $\rho \approx 0.85$, yet both yield the same $\bar{\Lambda} = 0.200$.

Figure 2: Bounded Variance — Class I Confirmed

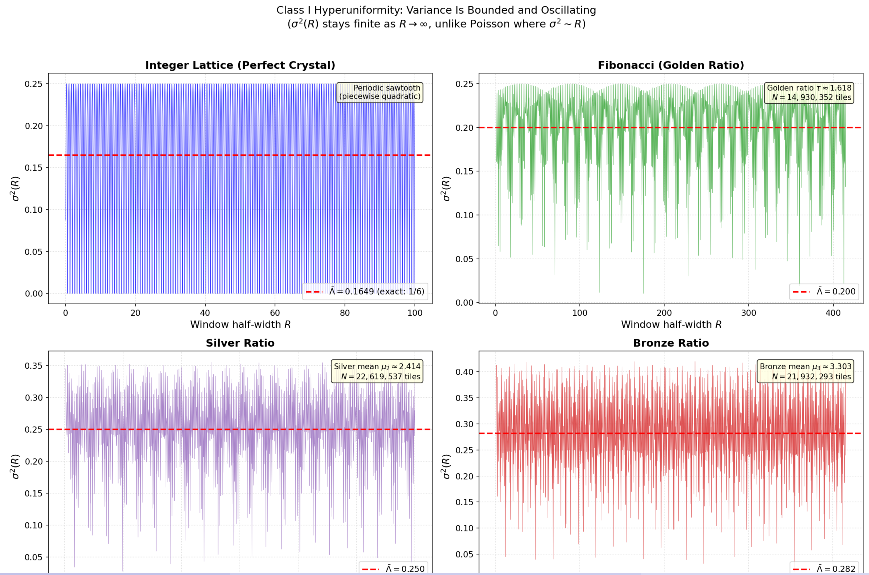

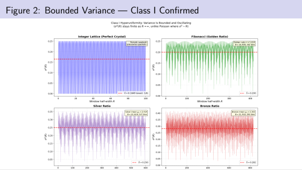

What this shows: Number variance $\sigma^2(R)$ for the integer lattice (top-left) and three quasicrystal chains. Each curve: 30,000 random windows at 1,000 R-values.

Key observation: All four curves are *bounded and oscillating* — they do not grow with R. This is the defining signature of Class I hyperuniformity.

Red dashed lines: $\bar{\Lambda}$ (surface-area coefficient). Lattice: $\bar{\Lambda} \approx 1/6$. Values increase monotonically with μ: Fibonacci (0.200) $<$ Silver (0.250) $<$ Bronze (0.282).

Interpretation: More "aperiodic" chains (higher μ) have larger fluctuation amplitudes, but all remain Class I.

Pattern	N (tiles)	$\bar{\Lambda}$	vs Lattice
Integer Lattice	100,000	0.165 ($\approx 1/6$)	reference
Fibonacci (substitution)	14,930,352	0.200	1.21×
Silver (substitution)	22,619,537	0.250	1.51×
Bronze (substitution)	21,932,293	0.282	1.71×
Fibonacci (projection)	220,161	0.200	1.21×

- $\bar{\Lambda}$ increases monotonically with metallic mean μ
- Substitution vs. projection agree to **0.1%** for Fibonacci

$\Rightarrow$ $\bar{\Lambda}$ is **density-independent** (rescaling invariance confirmed)

Surface-Area Coefficient $\bar{\Lambda}$
Pattern | N (tiles) | $\bar{\Lambda}$ | vs Lattice
Integer Lattice | 100,000 | 0.165 ($\approx 1/6$) | reference
Fibonacci (substitution) | 14,930,352 | 0.200 | 1.21×
Silver (substitution) | 22,619,537 | 0.250 | 1.51×
Bronze (substitution) | 21,932,293 | 0.282 | 1.71×
Fibonacci (projection) | 220,161 | 0.200 | 1.21×
$\bar{\Lambda}$ increases monotonically with metallic mean μ
Substitution vs. projection agree to **0.1%** for Fibonacci
$\Rightarrow$ $\bar{\Lambda}$ is **density-independent** (rescaling invariance confirmed)

The projection method generates Fibonacci at $\rho \approx 0.85$ while substitution gives $\rho \approx 0.72$. Despite the density difference, $\bar{\Lambda}$ agrees to 0.1%. Under rescaling $x \to ax$, we have $\sigma'^2(R) = \sigma^2(R/a)$ whose long-range average is unchanged. This numerical verification confirms the theoretical expectation.

Figure 3: Hyperuniformity Test — $\sigma^2(R)/R \to 0$

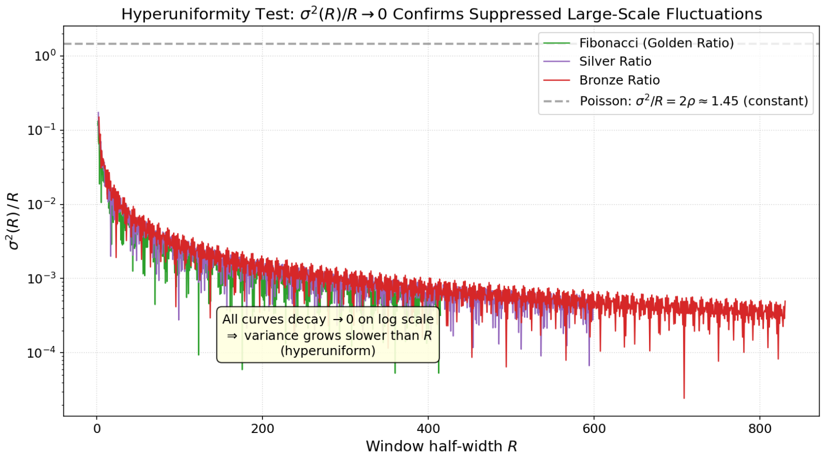

Figure 3: For random (Poisson) patterns, $\sigma^2/R = 2\rho =$ const. For hyperuniform patterns, this ratio vanishes.

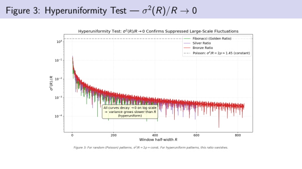

What this shows: The ratio $\sigma^2(R)/R$ on a log scale for all three chains. For Poisson, this ratio equals $2\rho \approx 1.45 =$ const (gray dashed line at top). For any hyperuniform pattern, it must decay to zero.

Key observation: On the log y-axis, the decay from $\sim 10^{-1}$ to $\sim 10^{-3}$ is clearly visible. All three chains show power-law–like decay, confirming that number fluctuations grow much slower than the window size.

Why it matters: This is the simplest direct real-space test of hyperuniformity. The three orders-of-magnitude gap between the Poisson constant and the quasicrystal curves at large R is the signature of suppressed fluctuations.

Figure 4: Projection — Class I vs. Class II

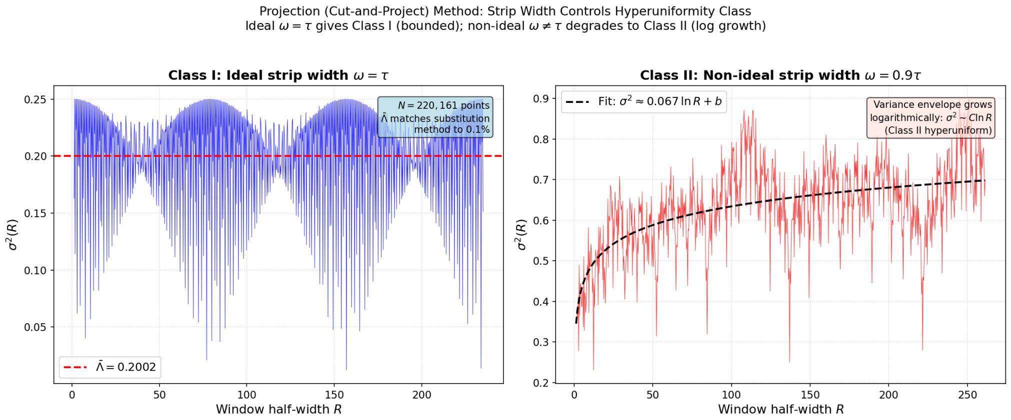

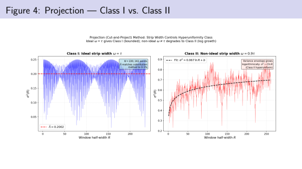

Left panel (Class I): Ideal strip width $\omega = \tau$. Variance is bounded with $\bar{\Lambda} = 0.200$, matching the substitution result to 0.1%.

Right panel (Class II): Non-ideal strip width $\omega = 0.9\tau$. The variance envelope *grows logarithmically*: $\sigma^2 \sim 0.067 \ln R + b$. This logarithmic growth is the hallmark of Class II hyperuniformity.

Takeaway: The hyperuniformity class is controlled by the projection strip width. Any deviation from the ideal $\omega = \mu$ degrades Class I to Class II.

Figure 5: Piecewise Quadratic Structure

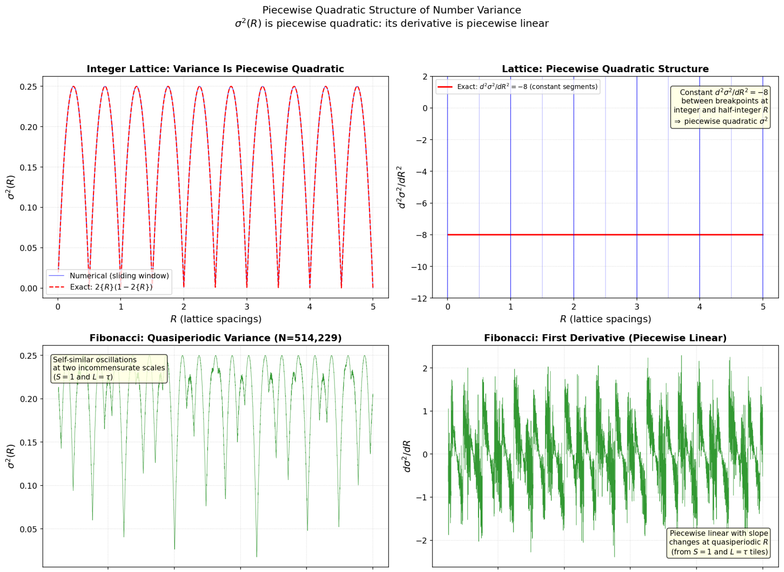

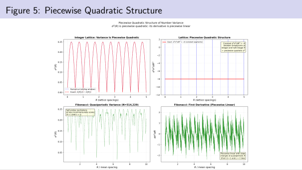

Top-left: Lattice variance at high resolution, overlaid with exact formula $\sigma^2(R) = 2\{R\}(1 - 2\{R\})$. Perfect agreement.

Top-right: The exact second derivative $d^2\sigma^2/dR^2 = -8$ is constant between breakpoints at every half-integer R. Vertical lines mark these breakpoints. This confirms σ^2 is piecewise quadratic.

Bottom-left: Fibonacci variance shows self-similar oscillations at two incommensurate scales (S=1 and L=τ).

Bottom-right: Fibonacci first derivative $d\sigma^2/dR$ is piecewise linear with slope changes at quasiperiodic positions determined by S and L tile lengths — confirming the piecewise quadratic structure with a dense set of breakpoints.

The Two-Phase Media Approach

Problem: $S(k)$ has dense Bragg peaks at irrational $k \implies$ cannot read off α directly.

Solution — four steps:

1. **Decorate** each point with a solid rod (half-length $a = \phi_2/2\rho$, $\phi_2 = 0.35$)
2. **Compute** spectral density: $\tilde{\chi}_V(k) = \rho\left(\frac{2\sin ka}{k}\right)^2 S(k)$
3. **Evaluate** excess spreadability: $E(t) = \frac{\Delta k}{\pi\phi_2}\sum_n \tilde{\chi}_V(k_n)\, e^{-k_n^2 Dt}$
4. **Extract** α from long-time decay: $\alpha(t) = -2\,\frac{d\ln E}{d\ln t} - 1$

Chain	ρ	Rod $2a$	Min gap	Overlap?
Fibonacci	0.724	0.484	1.000	No
Silver	0.500	0.700	1.000	No
Bronze	0.361	0.969	1.000	No

The Two-Phase Media Approach

Problem: $S(k)$ has dense Bragg peaks at irrational $k \implies$ cannot read off α directly.

Solution — four steps:

1. **Decorate** each point with a solid rod (half-length $a = \phi_2/2\rho$, $\phi_2 = 0.35$)
2. **Compute** spectral density: $\tilde{\chi}_V(k) = \rho\left(\frac{2\sin ka}{k}\right)^2 S(k)$
3. **Evaluate** excess spreadability: $E(t) = \frac{\Delta k}{\pi\phi_2}\sum_n \tilde{\chi}_V(k_n)\, e^{-k_n^2 Dt}$
4. **Extract** α from long-time decay: $\alpha(t) = -2\,\frac{d\ln E}{d\ln t} - 1$

Chain	ρ	Rod $2a$	Min gap	Overlap?
Fibonacci	0.724	0.484	1.000	No
Silver	0.500	0.700	1.000	No
Bronze	0.361	0.969	1.000	No

The two-phase media approach was introduced by Torquato (2021). The key insight: the Gaussian kernel $e^{-k^2 Dt}$ in the spreadability integral acts as a natural smoother of the Bragg peak spectrum. At time t, it samples wavevectors $k \lesssim 1/\sqrt{Dt}$. The power-law tail of the Bragg peak envelope then translates into a power-law decay of $E(t)$, from which α can be extracted.

Non-overlap is verified: $2a < \min(\text{spacings}) = 1.0$ for all chains. The packing fraction $\phi_2 = 0.35$ is chosen following Hitin-Bialus et al. (2024).

Figure 6: Spectral Density Reveals k^3 Scaling

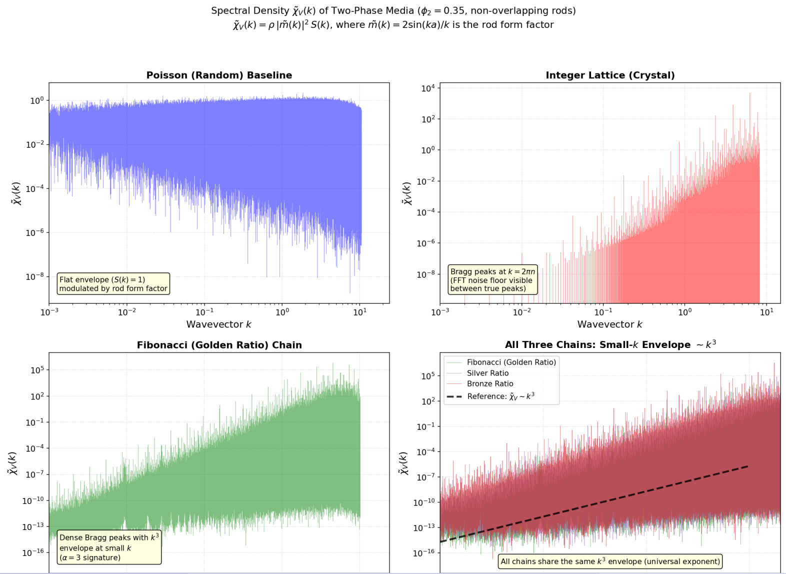

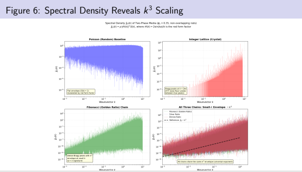

Top-left (Poisson): Flat $S(k) = 1$ envelope, modulated only by the rod form factor $|\tilde{m}(k)|^2$. No hyperuniformity.

Top-right (Lattice): Bragg peaks at $k = 2\pi n$. The FFT computation introduces a noise floor between the true peaks (this does not affect results since the lattice spreadability is computed analytically).

Bottom-left (Fibonacci): Dense Bragg peaks. The envelope of peak heights follows k^3 at small k — the spectral signature of $\alpha = 3$.

Bottom-right (All chains overlaid): All three chains share the same k^3 envelope (black dashed reference line), confirming universality.

The k^3 scaling is the Fourier-space manifestation of $\alpha = 3$ Class I hyperuniformity.

Figure 7: Excess Spreadability — Decay Rates

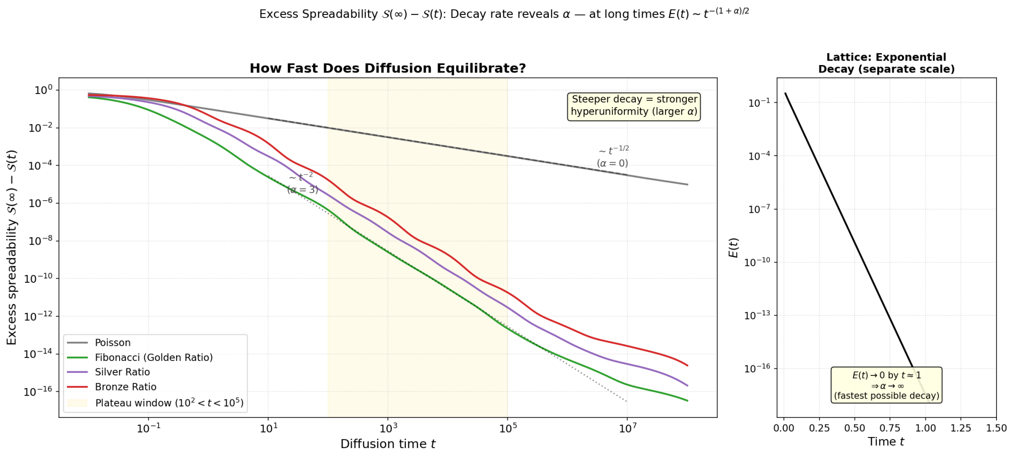

At long times: $E(t) \sim t^{-(1+\alpha)/2}$. More hyperuniform = faster equilibration.

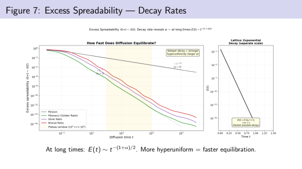

Main panel (left): Log-log plot of excess spreadability $E(t)$ for Poisson and the three quasicrystals.

Gray (Poisson): Slow decay $\sim t^{-1/2}$ $(\alpha = 0)$.

Green/Purple/Red (quasicrystals): Steeper decay $\sim t^{-2}$ $(\alpha = 3)$. The gold shaded region marks the measurement window $[10^2, 10^5]$.

Right panel (Lattice): Plotted on separate axes because the lattice $E(t)$ decays *exponentially* (reaches zero by $t \approx 1$), confirming $\alpha \to \infty$. If plotted on the same axes, it would compress all other curves to a thin band.

Hierarchy: Random $<$ quasicrystal $<$ crystal in terms of equilibration speed.

Main Result: All Three Chains Converge to $\alpha = 3$

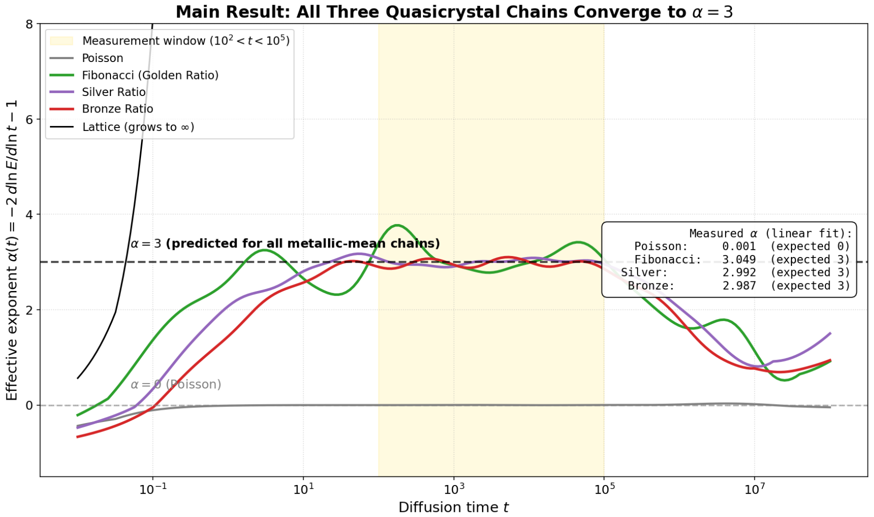

Figure 8: α extracted via period-aware log-derivative (curves) and linear fit of $\ln E$ vs $\ln t$ (reported values). Plateau at $\alpha = 3$ confirms Class I hyperuniformity.

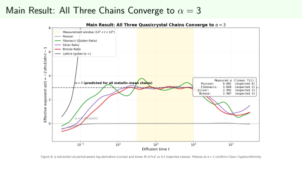

This is the central result of the project.

The effective exponent $\alpha(t) = -2\, d \ln E / d \ln t - 1$ is plotted versus diffusion time t. Smoothing uses a period-aware sliding window matched to each chain's oscillation period $2 \ln \mu$ in $\ln t$ space (cancels oscillatory contributions).

Gray (Poisson): Flat at $\alpha \approx 0$ — correct.

Black (Lattice): Grows without bound — $\alpha \to \infty$.

Green/Purple/Red: All plateau at $\alpha \approx 3$ within the gold-shaded measurement window $[10^2, 10^5]$.

Measured values (linear fit of $\ln E$ vs $\ln t$): Poisson $= 0.001$, Fibonacci $= 3.049$, Silver $= 2.992$, Bronze $= 2.987$.

All three metallic-mean chains confirm $\alpha = 3$ via an independent dynamical measurement, matching the eigenvalue prediction.

Extracted α Values

Pattern	α (measured)	Expected	Status
Poisson	0.001	0	✓
Integer Lattice	exp. decay	∞	✓
Fibonacci (Golden Ratio)	**3.049**	**3**	✓
Silver Ratio	**2.992**	**3**	✓
Bronze Ratio	**2.987**	**3**	✓

All three metallic-mean chains yield $\alpha \approx 3$, confirming the universal eigenvalue prediction via an independent dynamical measurement (diffusion spreadability).

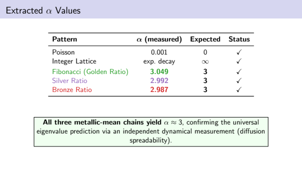

Values extracted via linear fit of $\ln E$ vs $\ln t$ over $[10^2, 10^5]$ (more robust than pointwise median, averages over oscillations). Errors: Fibonacci 1.6%, Silver 0.3%, Bronze 0.4%. These are consistent with finite-size effects from the FFT grid.

The two benchmarks (Poisson $\alpha = 0$ and lattice $\alpha \to \infty$) bracket the quasicrystal results and confirm the method is working correctly at both extremes.

Technical Challenges & Solutions

1. System size sensitivity (non-monotonic convergence):

- FFT grid $k_n = 2\pi n/L$ misaligns with irrational Bragg peaks
- Fibonacci (ρ=0.72, smallest L for given N) needs $N \sim 10^7$
- Convergence is *non-monotonic*: N=500k gives α=1.5, N=5.7M gives α=1.5, N=14.9M gives α=3.0

2. Integer lattice artifact:

- FFT histogram binning creates noise floor mimicking $k^3 \Rightarrow$ spurious $\alpha \approx 3$
- **Fix:** analytical Bragg peak formula $E(t) = \frac{2\rho}{\phi_2} \sum_{n=1}^{50} |\tilde{m}(2\pi n)|^2 e^{-(2\pi n)^2 Dt}$

3. Noisy log derivative:

- Point-by-point `np.gradient` amplifies Bragg peak noise
- **Fix 1:** Period-aware sliding window matched to oscillation period $2\ln\mu$ (cancels oscillatory contributions)
- **Fix 2:** Linear fit of $\ln E$ vs $\ln t$ over plateau window for single robust α value

Technical Challenges & Solutions
1. System size sensitivity (non-monotonic convergence):
FFT grid $k_n = 2\pi n/L$ misaligns with irrational Bragg peaks
Fibonacci (ρ=0.72, smallest L for given N) needs $N \sim 10^7$
Convergence is non-monotonic: N=500k gives α=1.5, N=5.7M gives α=1.5, N=14.9M gives α=3.0
2. Integer lattice artifact:
FFT histogram binning creates noise floor mimicking $k^3 \Rightarrow$ spurious $\alpha \approx 3$
Fix: analytical Bragg peak formula $E(t) = \frac{2\rho}{\phi_2} \sum_{n=1}^{50} |\tilde{m}(2\pi n)|^2 e^{-(2\pi n)^2 Dt}$
3. Noisy log derivative:
Point-by-point np.gradient amplifies Bragg peak noise
Fix 1: Period-aware sliding window matched to oscillation period $2\ln\mu$ (cancels oscillatory contributions)
Fix 2: Linear fit of $\ln E$ vs $\ln t$ over plateau window for single robust α value

These challenges consumed the majority of the Phase 4 development time. The non-monotonic convergence was the most surprising finding: certain system sizes give *worse* results than smaller ones because of how the FFT grid happens to align (or misalign) with the dominant Bragg peaks. Fibonacci is the hardest case because its high density ($\rho = 0.72$) means the smallest domain L for a given N, and hence the coarsest k-resolution. Silver and Bronze converge at $N \sim$ 2–4M.

Summary of All Results

Real-space analysis (Phases 1–3):

- Variance code validated against Poisson exact result (1.8% error)
- Class I hyperuniformity confirmed: bounded $\sigma^2(R)$ for all chains
- $\bar{\Lambda}$ increases with μ: 0.200 (Fib) $<$ 0.250 (Ag) $<$ 0.282 (Br)
- Rescaling invariance: substitution vs. projection agree to 0.1%
- Class I $\to$ II transition demonstrated via non-ideal strip width

Reciprocal-space analysis (Phase 4):

- $\tilde{\chi}_V(k) \sim k^3$ envelope confirmed for all chains
- Spreadability decay: Poisson $t^{-1/2}$, quasicrystal t^{-2}, lattice exp.
- $\alpha = 3.0 \pm 0.05$ **for all three chains** (linear fit method)

$\alpha = 3$ is a **universal property** of all metallic-mean 1D substitution tilings, confirmed both *analytically* (eigenvalue formula) and *numerically* (spreadability).

This slide summarizes all findings across four phases.
The key narrative: we approached the same question ($\alpha = 3$?) from two completely independent directions — real-space variance analysis and reciprocal-space spreadability — and both confirm the theoretical prediction. The agreement across three distinct quasicrystal families with different metallic means provides strong evidence for universality.

Future Work: Phase 5 — 2D Extensions

Planned:

- Construct 2D quasiperiodic tilings via the **Generalized Dual Method (GDM)**:
  - 5-fold Penrose tiling (golden ratio) — $\alpha = 6$ known
  - 8-fold octagonal tiling (silver mean) — α **unknown**
  - Bronze-ratio equivalent — α **unknown**
- Decorate vertices with disks ($\phi_2 = 0.25$)
- Compute 2D radial spectral density and extract α

Open questions:

1. Is $\alpha = 6$ universal for all 2D metallic-mean tilings (analogous to $\alpha = 3$ in 1D)?
2. Does the eigenvalue formula generalize correctly to 2D inflation matrices?
3. How large must 2D systems be for convergence?

The 2D Penrose tiling has $\alpha = 6$ from the literature. The eigenvalue formula for 2D inflation matrices predicts $\alpha = 6$ for Penrose, but the predictions for silver-mean and bronze-mean 2D tilings have not been tested numerically.

Based on the 1D experience, system size requirements may be substantial and non-trivial. The GDM provides a systematic way to generate arbitrary *n*-fold tilings.

Appendix: Code & Reproducibility

File	Purpose
`substitution_tilings.py`	Chain generation (3 metallic means)
`projection_method.py`	Cut-and-project from $\mathbb{Z}^2$
`quasicrystal_variance.py`	Number variance + $\bar{\Lambda}$
`two_phase_media.py`	Spectral density + spreadability
`run_all.py`	Full pipeline: Figs 1–8 + tables

Reproducibility: `python run_all.py`

- Deterministic (seed = 42)
- Runtime: $\sim$18 minutes
- Generates all 8 figures + summary tables
- Dependencies: NumPy, Matplotlib, SciPy

Appendix: Code & Reproducibility
File | Purpose
substitution_tilings.py | Chain generation (3 metallic means)
projection_method.py | Cut-and-project from $\mathbb{Z}^2$
quasicrystal_variance.py | Number variance + $\bar{\Lambda}$
two_phase_media.py | Spectral density + spreadability
run_all.py | Full pipeline: Figs 1–8 + tables
Reproducibility: python run_all.py
Deterministic (seed = 42)
Runtime: $\sim$18 minutes
Generates all 8 figures + summary tables
Dependencies: NumPy, Matplotlib, SciPy

All code is self-contained in five Python files. The full pipeline is run with a single command and is fully deterministic.

The bottleneck is the Phase 4 FFT computation for the three quasicrystal chains at $N \sim 10^7$ (about 5 minutes each for Silver and Bronze due to larger FFT sizes).